Microscopic assessment of ASR-affected columns after 20 years in service

Hesham Ahmed[1], *Andisheh* Zahedi[1,*], and *Leandro* Sanchez[1]

[1]University of Ottawa, Ottawa, Canada

Abstract. Deterioration signs were observed on the concrete surface of the exterior columns of the SITE building located at the University of Ottawa, Ottawa (Ontario, Canada) which demonstrated the potential presence of a concrete damage mechanism, suspected to be alkali-silica reaction (ASR). To investigate the root cause of this deterioration, a visual inspection was conducted to select concrete members for coring. Damage development in the extracted cores was then evaluated through various microscopic techniques to identify the cause and extent of deterioration. First, the petrographic examination was carried out with the aim of detecting the cause of damage in the extracted core specimens through the analysis of damage features; confirming the presence of ASR in the selected elements Afterwards, the Damage Rating Index (DRI), a semi-quantitative microscopic procedure, was used to evaluate the extent of the damage. Data collected during the visual inspection and petrographic examination will be presented and analyzed. Moreover, based upon the analysis of DRI results, the induced expansion levels in affected columns will be discussed, along with potential implications on their structural performance.

1 Introduction

Having been discovered in over 50 countries around the world, Alkali-silica reaction (ASR) is one of the leading causes of concrete distress, resulting in loss of serviceability in affected structures [1]. ASR occurs when un/poorly crystallized silica in reactive aggregates reacts with alkali hydroxides present in the concrete pore solution, resulting in the production of a viscous secondary reaction product known as "ASR gel" or "silica gel" [1,2]. Upon exposure to moisture, the above-mentioned reaction product swells and resulting in concrete cracking and expansion, leading to the degradation of mechanical properties in affected structures. Over the last few decades, many structures have been discovered presenting ASR distress signs (e.g., [3,4]), including a reduced capacity for resisting service loads, resulting in significant concerns about public safety [5,6]. To ensure adequate structural integrity and the selection of effective rehabilitation measures, the condition assessment of aging structures is critical [7,8].

Several methods for the appraisal of ASR damage (diagnosis) as well as the potential for further deterioration (prognosis) of deteriorated elements have been developed recently [9]. Among those, the Damage Rating Index (DRI), a semi-quantitative microscopic procedure has shown to be very reliable to evaluate the extent of damage in deteriorated concrete [10]. Despite originally being developed in a laboratory setting (i.e., under free expansion), DRI analysis has been successfully used to appraise restrained concrete specimens [9,11] as well as distinct structural members in field conditions [3,8].

Therefore, this work tried to use such microscopic testing procedure to appraise the condition of the external columns of the School of Information Technology and Engineering (SITE) building at the University of Ottawa (Ottawa, ON, Canada) that has been in service for around 20 years (Figure 1). Although the cause(s) and extent of damage is unknown, surface deterioration signs such as map cracking surrounded by 'dark rims' of moisture, exudation of whitish products on the surface of concrete columns as well as spalling and surface scaling (Figure 2) indicate that ASR could potentially be involved. Thus, in order to assess the condition of those deteriorated elements, initially, visual inspection was conducted to evaluate overall surface deterioration across members. Next, cores were extracted from select columns with the highest sign of visual deterioration for microscopic evaluations including petrographic examination and DRI analysis. Finally, results were used to determine the cause(s) and extent of deterioration in the columns.

Figure 1. *External rotunda columns of the S.I.T.E. building.*

* Corresponding author: azahe049@uottawa.ca

Figure 2. *External rotunda columns of the S.I.T.E. building.*

2 Condition assessment tools for ASR damage

2.1. Visual inspection

Visual inspection is commonly the first analytical procedure conducted during the condition assessment of deteriorated structures [12,13]. One of the most commonly used techniques for conducting the visual inspection is the cracking index (CI) method [14], which aims to assess the visual integrity of deteriorated concrete quantitatively. Conventionally, the procedure for determining the CI begins with constructing a 0.5x0.5m grid as shown in Figure 3, and then measuring crack widths intercepting each interval using a crack comparator card. Finally, the CI can be calculated through the eq. 1 as the ratio of total measured crack widths per unit length, where "Σ crack opening" represents the sum of all crack widths measured across a "base length" 0.5m:

$$CI = \frac{\sum crack\ opening}{Base\ length} \quad (1)$$

As per Fournier et al. [15], normally, concrete members displaying CI values above 0.5 mm/m and crack widths greater than 0.15 mm (on average) require further appraisal through mechanical and/or microscopic testing procedures.

The CI procedure was implemented for the visual inspection of the SITE building columns, where the evaluation was performed on the most 'damaged' face of each member to enable a viable comparison of damage levels among all 15 columns. Coring was then performed in the "four" most deteriorated columns through the use of 100-mm hydraulic drills to extract two horizontal specimens (roughly 730mm and 830mm in length) across the widths of each member. Finally, the cores were promptly wrapped and stored in an environmentally controlled chamber at 12°C ± 2°C as per [16] to halt any ongoing reactions, before being cut into 200mm specimens using a diamond-bladed concrete saw.

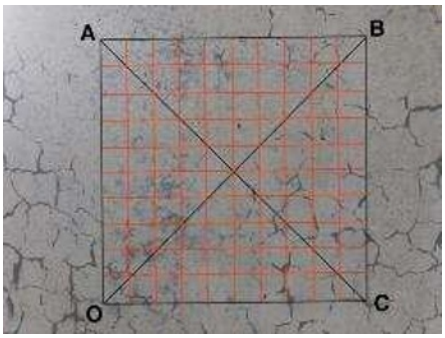

Figure 3. *Cracking Index (CI) grid on the S.I.T.E. column.*

2.2 Petrographic examination

Normally, petrographic examination is the first test conducted on thin sections using a petrographic microscope. Typically, distress features associated with ASR damage (i.e., ASR-induced cracks in coarse/fine aggregates and potential ASR gel) are investigated with the aim of confirming ASR as the main cause (or one of the causes) of concrete distress. As a supplement, this analysis is commonly coupled with EDX/SEM (i.e., energy dispersive x-ray and scanning electron microscopy) to reveal the constituency and morphology of aggregates, cement paste, and reaction products.

Thus, the petrographic examination was conducted on thin sections (i.e., 75x50mm) prepared from the cores extracted from the damaged column in order to investigate the cause of the deterioration in the damaged columns.

2.3 Damage Rating Index (DRI)

DRI is a semi-quantitative microscopic procedure used to assess the extent of damage in affected concrete, was initially developed by Grattan-Bellew and coworkers in 1992 [10]. This analysis is carried out on a 100x200mm specimens using a petrographic microscope under a 15-16X magnification with the objective of counting individual distress features in 1cm by 1cm grids drawn on the surface of polished concrete and multiplying them by their relevant weighting factor (as shown in Table 1), whose purpose is to balance the overall deterioration of the concrete [17]. Finally, the DRI number is determined by summing up the weighted count of all distress features and normalizing the result to 100 cm^2 to provide a measure of the degree of ASR damage.

DRI analysis was conducted on three samples per column after each sample was cut longitudinally and then polished using grits 30, 60, 140, 280, 600, 1200, and 3000 to produce a clear surface. Prior to the examination, a 1x1cm grid was hand-drawn on the surface of polished concrete to facilitate the counting of petrographic features.

Table 1. DRI weighting factors [17].

Petrographic features	Weighting factors
Closed cracks in aggregates (CCA)	0.25
Opened cracks in aggregates (OCA)	2
Opened crack with reaction product in aggregate (OCAG)	2
Coarse aggregate de-bonded (CAD)	3
Disaggregate/corroded aggregate particle (DAP)	2
Cracks in cement paste (CCP)	3
Cracks with reaction product in cement paste (CCPG)	3

3 Results and discussion

3.1 Visual inspection

Figure 4 presents values of the CI and average crack widths recorded for all external columns. Columns C1, C2, C3, C4, C7, and C11 were all found to have a CI > 0.5 mm/m and average crack widths > 0.15 mm, justifying further laboratory investigation using core-based testing methods. Nevertheless, the four columns presenting the greatest distress features (i.e., C1, C3, C4, and C7 - highest values of CI and crack width) were selected for coring. Furthermore, damage ratings of 'very high' and 'high' were assigned to C3/C4 and C1/C7, respectively, based on recorded measurements and qualitative distress features.

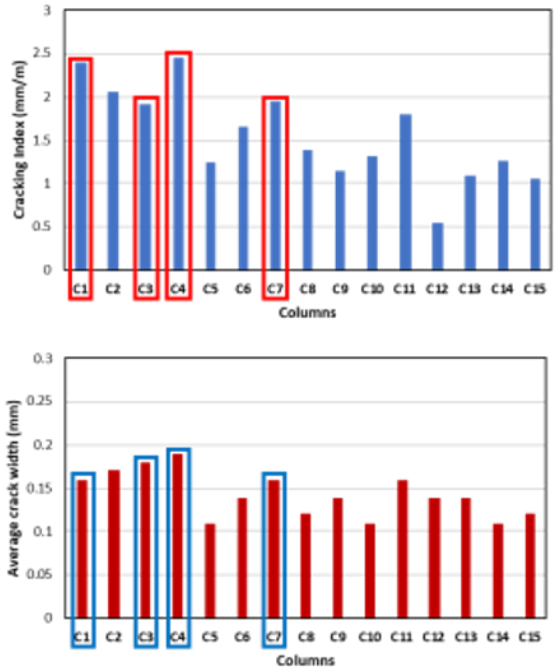

Figure 4. *Top: Measured cracking index (CI) and bottom: average crack width (mm) of each column of SITE building.*

3.2 Petrographic examination

Upon the examination of the thin section specimens, various cracks were observed both in the coarse aggregate particles and cement paste of the majority of the specimens, mostly originating from coarse aggregates (Figure 5). Furthermore, according to the results obtained through the petrographic analysis, ASR gel was found in the coarse aggregate and the cement paste cracks (Figure 6). As per the petrographic examination performed on the concrete specimens, various distress features associated with ASR including cracks in coarse aggregates, and the presence of reaction products (i.e., ASR gel) in the coarse aggregate particles, cement paste and cement paste voids clearly confirmed the presence of ASR in the SITE building.

Figure 5. *Crack in the coarse aggregate, 25X, natural light.*

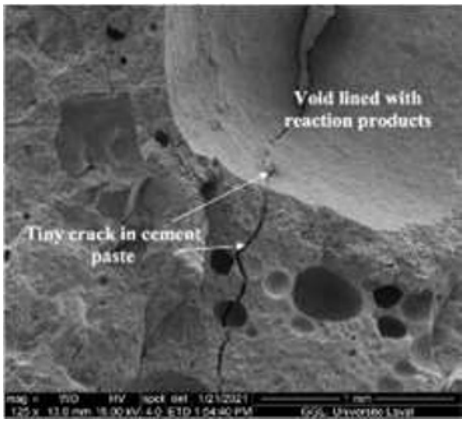

Figure 6. *Crack in cement paste and void lined with reaction products observed at SEM (secondary electron picture).*

3.3 Damage Rating Index (DRI)

Figure 7 presents the results of the DRI analysis conducted on extracted core specimens. Observing the chart, one notices that the most outstanding features include closed cracks in reactive aggregates (i.e., CCA – blue bar), open cracks in reactive aggregates (i.e., OCA – red bar), and cracks in the cement paste (i.e., CCP – orange bar). However, it is worth noting that CCA is often considered not to be a sign of damage mechanisms, but rather caused by weathering or manufacturing procedures such as crushing or sieving. Evidently, a similar extent of CCA was observed in all specimens (i.e., C1=120, C3=129, C4=100, C7=110). On the other hand, varying amounts of OCA were observed, with the highest number present in C4 (i.e., 132), followed by C3 (i.e., 76), and C1/C7 (i.e., 46). Similarly, the highest number of CCP was visible in C4 (i.e., 88), followed by C3 (i.e., 45), C1 (i.e., 21), and C7 (i.e., 20). Although present in small amounts, open cracks with reaction products (OCAG –

green bar in Figure 7) were identified in C4 (i.e., 51) and C3 (i.e., 14) whereas cracks in cement paste with gel (CCPG – light blue bar in Figure 7) were observed in C4 (i.e., 9). Evidently, C4 (i.e., 381) presented the highest DRI number, followed by C3 (i.e., 265), C1 (i.e., 187), and C7 (i.e., 176).

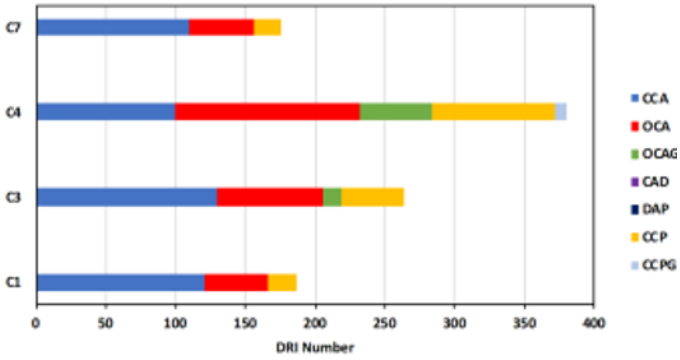

Figure 7. *Results of Damage Rating Index.*

Analyzing the results gathered from the DRI, similar to the petrographic analysis, the presence of ASR could be attested through this method. As such the observation of open cracks with and without reaction product (i.e., OCAG and OCA, green and red chart in figure 7) along with the presence of cement paste cracks with reaction product (i.e., CCPG, light blue chart in figure 7) could confirm the above. Figure 8 displays the above features in examined specimens.

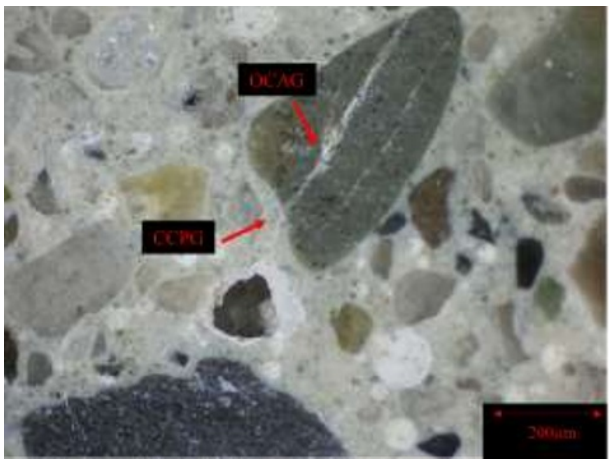

Figure 8. *Presence of open crack in aggregate and cement paste crack with ASR reaction product.*

In order to further investigate the extent of ASR-induced damage (i.e., expansion), the results obtained in this study were compared with the DRI protocol that was previously proposed by Sanchez et al. [16,18]. Such protocol was developed with a confidence level of 95% based on a micro-mechanical coupling of ASR damage features through a comprehensive laboratory testing program that incorporated mix designs with 13 different reactive aggregates and 3 different concrete strengths (i.e., 25, 35, and 45MPa) [16,18]; the resulting table (i.e., Table 2) could help to find the extent damage in ASR-affected concrete elements [16,18]. Finally, despite being developed using laboratory specimens under "free-expansion" conditions, it is worth noting that this protocol has been shown to reliably assess the damage level of ASR-damaged concrete in the field and under confined conditions [3,8,19,20].

Table 2. Correlation of ASR damage degree, expansion levels and the results of microscopic assessment [16].

ASR damage degree (%)	Reference expansion level (%)[1]	Multi-level assessment	
		SDI	DRI
Negligible	0.00 – 0.03	0.06 – 0.16	100 - 155
Marginal	0.04 ± 0.01	0.11 – 0.25	210 - 400
Moderate	0.11 ± 0.01	0.15 – 0.31	330 - 500
High	0.20 ± 0.01	0.19 – 0.32	500 - 765
Very High	0.30 ± 0.01	0.22 – 0.36	600 – 925

The above chart can generally be used to appraise damage in one of two ways: 1) by selecting the damage envelope of a similar aggregate to the one under assessment, or 2) by averaging out the data for two different aggregates, if the one under assessment is not represented in the chart [3,16]; the second option has been adopted in this work in order to find the degree of ASR damage and expansion induced in each concrete columns which were appraised in this study.

Comparing the DRI results gathered in this study and those DRI range proposed by Sanchez et al. [16,18], the following result has been obtained: the greatest level of distress was found in C4 (i.e., moderate – 0.08%), followed by C3 (i.e., marginal - 0.05), and C1/C7(i.e., negligible – 0.03%). These results can be seen in Figure 9.

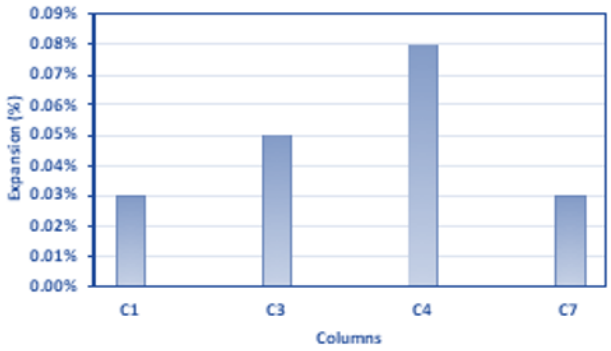

Figure 9. *Potential expansion attained for assessed columns.*

According to the induced expansion result (Figure 9), the damage level is at the negligible/low stage, therefore, the reaction is in the early stages. no immediate structural implications are foreseeable for the examined members, particularly due to the negligible loss in compressive strength (i.e., the predominant type of loading exerted on the columns) exhibited at the aforementioned expansion levels. One may predict that such losses may become more pronounced in the long-term (i.e., within 10 years) as the expansion levels rise beyond moderate levels (i.e., ≈ 0.10 to 0.12%) [16]. It is worth noting that the induced expansion of concrete columns is in accordance with the

observation made on the petrographic analysis where very limited ASR products were detected in thin section specimens which suggests that the damage level is negligible/low stage.

3.4 Comparison of the visual inspection result with induced expansion

Upon comparing the level of ASR damage characterized by visual inspection and microscopic assessment in Table 3, some interesting trends can be noted. The CI values appear to be associated with higher damage determined through multi-level assessment, where C4 (i.e., CI = 2.45 and 0.08% expansion) was characterized as the most damaged, and C1/C7 (i.e., CI = 2.07/1.95 and 0.03% expansion) as the least damaged. Nevertheless, despite the potentially diagnostic characteristic of visual inspection, it can often mischaracterize the extent of ASR damage. As shown in a previous study by [3], this effect could be attributed to two main reasons: 1) the inability to clearly differentiate two different levels of damage, and 2) the tendency of visual inspection to overestimate deterioration. Moreover, conflicting observations were made by researchers when implementing visual inspection in laboratory (i.e., underestimated damage – by as much as 40%) and field settings (i.e., overestimated damage) [21–25], possibly due to the contribution of external exposure conditions. This unreliable characteristic associated with visual inspection techniques emphasizes the importance of core-based evaluations and methods such as the Damage Rating Index (DRI) in evaluating the internal level of damage in affected concrete.

Table 3. Comparison between visual inspection and the induced expansion.

	Visual Inspection			Microscopic assessment		
Column	CI (mm/m)	Average crack width (mm)	Damage Degree	Expansion (%)	Damage Degree	Classification (✓/X)
C1	2.07	0.16	High	0.03	Minimal	X
C3	2.40	0.18	Very High	0.05	Marginal	X
C4	2.45	0.19	Very high	0.08	Moderate	X
C7	1.95	0.16	High	0.03	Minimal	X

4 Conclusion

This work focused on the condition assessment of deteriorated columns (located in the SITE building in Ottawa, Canada) using visual inspection and microscopic assessment (Damage Rating Index-DRI) after around 20 years in service. The following conclusions can be deduced from this work:

- The result of visual inspection demonstrates that all concrete columns of this work displayed various signs of damage including map cracking, surface spalling and scaling which could be the sign of ASR damage.

- After obtaining core specimens from the four columns that showed the highest sign of damage during the visual inspection, a petrographic assessment was conducted on those specimens. As a result of such analysis, ASR-induced damage was confirmed in all appraised specimens, where a number of cracks were observed both in the coarse aggregate particles and cement paste of the majority of the specimens, mostly originating from coarse aggregates Particles. Moreover, the signs of ASR product were found in the coarse aggregate and the cement paste cracks of most concrete specimens.

- Despite their close physical proximity, the microscopic assessment of all columns demonstrated varying degrees of damage, with the most damaged column being C4 (i.e., moderate - 0.08%), followed by C3 (i.e., marginal – 0.05%), and C1/C7 (i.e., negligible – 0.03%). According to the above result, no immediate structural implications exist within the columns as a result of ASR-induced damage.

- No correlation was found between visual inspection and microscopic assessment procedure, as the former was found to only be useful for detecting the potential presence of ASR-induced damage yet it is unable to demonstrate the extent of damage in various concrete elements of this study.

References

[1] B. Fournier, M.A. Bérubé, Can. J. Civ. Eng. **27** (2000).

[2] F. Rajabipour, E. Giannini, C. Dunant, J.H. Ideker, M.D.A. Thomas, Cem. Concr. Res. **76** (2015).

[3] L.F.M. Sanchez, B. Fournier, D. Mitchell, J. Bastien, Constr. Build. Mater. **236** (2020).

[4] M.A. Berube, B. Durand, D. Vézina, B. Fournier, Can. J. Civ. Eng. **27** (2000).

[5] A. Shayan, A. Xu, F. Andrews-Phaedonos, Road Transp. Res. **24** (2015).

[6] B.P. Gautam, D.K. Panesar, S.A. Sheikh, F.J. Vecchio, N. Orbovic, (2015).

[7] V.E. Saouma, *Diagnosis & prognosis of AAR affected structures: state-of-the-art report of the RILEM Technical Committee,* (2021).

[8] B. Fournier, M.A. Berube, K.J. Folliard, M. Thomas, Report on the Diagnosis, Prognosis, and Mitigation of Alkali-Silica Rection (ASR) in Transportation Structures, Austin, (2010).

[9] A. Zahedi, C. Trottier, L.F.M. Sanchez, M. Noel, Cem. Concr. Res. **153** (2022).

[10] L.F.M. Sanchez, B. Fournier, M. Jolin, J. Duchesne, Cem. Concr. Res. **67** (2015).

[11] A. Zahedi, C. Trottier, L. Sanchez, M. Noël, Cem Concr Res. (2021).

[12] S. Kashif, U. Rehman, Z. Ibrahim, S. Ali, M. Jameel, Constr. Build. Mater. **107** (2016).

[13] A. Zahedi, L.F.M. Sanchez, M. Noël, Constr. Build. Mater. **323** (2022).

[14] B. Godart, P. Fasseu, M. Michel, *9th Int. Conf. Alkali-Aggregate React. Concr.* (1992).

[15] B. Fournier, A. Bérubé, J. Folliard, M. Thomas, Report No. FHWA-HIF-09-004, Federal Highway Administration, U. S. Department of Transportation, (2010).

[16] L.F.M. Sanchez, B. Fournier, M. Jolin, D. Mitchell, J. Bastien, Cem. Concr. Res. **93** (2017).

[17] V. Villeneuve, B. Fournier, *14th ICAAR — Int. Conf. Alkali– Aggreg. React. Concr*., (2012).

[18] L.F.M. Sanchez, T. Drimalas, B. Fournier, D. Mitchell, J. Bastien, Cem. Concr. Res. **107** (2018).

[19] M.D.A. Thomas, K.J. Folliard, B. Fournier, P. Rivard, T. Drimalas, S.I. Garber, Final Report, Fed. Highw. Adm. FHWA-HIF-1 (2013).

[20] R. Rivard, Quantitative Petrographic Technique for Concrete Damage Due to ASR : Experimental and Application, (2000).

[21] M. Bérubé, N. Smaoui, B. Fournier, B. Bissonnette, B. Durand, Can. J. Civ. Eng. **32** (2005).

[22] A.E.K. Jones, L.A. Clark, *Inst. Civ. Eng. Struct. Build.* **104** (1994).

[23] N. Smaoui, M.A. Bérubé, B. Fournier, B. Bissonnette, B. Durand, Can. J. Civ. Eng. **30** (2004).

[24] N. Smaoui, B. Fournier, M. Bérubé, B. Bissonnette, B. Durand, Can. J. Civ. Eng. **31** (2004).

[25] D.J. Deschenes, The University of Texas at Austin, University of Texas, (2009).